Mechanical Properties of Needle-Punched Fabrics in Relation to Fiber Orientation

Reza Saghafi, Mohammad Zarrebini, and Meysam Moezzi

***Abstract*— Needle-Punching process is a mechanical method by which entanglement of fibrous webs can be enhanced. Fiber entanglement together with fabric weight can be held responsible for the variations in the mechanical properties of nonwovens. In this work, mean fiber orientation angle and fabric weight measurements were used for prediction of bending and tensile properties of needle-punched fabrics. Samples of needled nonwoven fabrics in four groups with different fabric weights were produced using appropriate carding/cross-lapping machines. The samples of each weight group were needled at various punch densities and needle penetration depths. The orientation of the fibers in the samples was determined using Radon transform method. Bending stiffness and breaking strength of the samples in both machine-direction and cross-machine direction were determined using two simply supported beam system and strip method, respectively. The results indicated that an increase in the amount of punch-density generally leads to variation in orientation angle of the fibers in the samples. It was observed that an increase in the amount of punch-density led to an increase in mean fiber orientation angle in all samples along the machine-direction. This is due to the displacement of the fibers by the needling process. Additionally, fiber orientation pattern of the samples enormously changed due to the changes in needle penetration depth. Multiple regressions based on least square method were used to estimate the mechanical properties of needle-punched fabrics. The results pointed to the paramount importance of the degree of fiber orientation and fabric weight as two influential factors controlling the mechanical properties of needle punched fabrics.**

Keywords: **bending modulus, breaking strength, fabric weight, mean fiber orientation angle, Radon transformation**

I. Introduction

In comparison to woven fabrics, non-woven fabrics present several advantages, such as lower production cost, higher bulkiness, superior hydraulic properties and thermal isolation ability. Needled nonwoven fabrics are produced by interlocking and re-orientation of fibers in fibrous webs by mechanical means. This mechanical interlocking is achieved by the action of felting needles that pass through the thickness of the web usually at a right angle.

The needling operation parameters such as punch-density, needle-penetration depth and type of needle affect the resultant fabric both physically and mechanically. Thus manipulation of these parameters and the specifications of the constituent fibers are the means by which the required functions in the fabric can be achieved. Variations in the fiber morphological parameters such as fiber orientation, curl, and fineness affect the mechanical behavior and the failure mechanism of these fabrics. Needled fabrics are engineered according to their end-use. Goswami *et al.* [1] studied the effect of fiber geometry on the punching-force characteristics during needle felting and showed that, the tensile behavior of needled fabrics is affected by arrangement of fibers within the fabric. Various methods have been used for evaluation of fiber orientation in non-woven fabrics. In this regard Pourdeyhimi *et al.* [2-6] used direct tracking, Fourier transform and flow field analysis together with image processing technique. Bugao and Ling [7] pioneered the use of Hough transform techniques to determine fiber orientation distribution in non-woven fabrics.

In the current study samples of needled nonwoven fabrics in four groups with different weights were produced using an appropriate carding/cross-lapping machine. Fiber orientation of the samples was determined using the novel Radon transform method. The breaking strength and bending modulus of the samples were determined using two simply supported beam system and strip method, respectively. Multiple regression method was used to investigate the effect of mean fiber orientation and fabric weight on the mechanical properties of the samples.

II. Materials and Methods

A. Production of Needle-Punched Samples

To produce needle punched fabrics, 12 dtex 90 mm long staple Polypropylene fibers with a crimp frequency of 3 crimps per centimeter were used. Four samples of continuous web with weights of 200, 300, 400 and 500 g m^{-2} were produced using an appropriate non-woven carding and horizontal cross-lapper system. The Groz-Beckert barb needles with the code of $15 \times 18 \times 38 \times 3$ R222 G3027 were used in the needling process. The samples were needled at punch-densities of 33, 42, 51, 60 and 66 punches per cm^2 using a needle penetration depth of 0, 7, 13 and 20 mm.

B. Radon Transform Method

The Radon transform function (Matlab toolbox) can be used to determine the fiber orientation of nonwovens [8]. In order to determine the fiber orientation of the samples a Visual Basic based computer program was developed. This program provided simulated images comprised of lines with different thicknesses lying in various directions. Fig. 1 shows three simulated images with lines at angles of

R. Saghafi and M. Moezzi are with the Department of Textile Engineering, Engineering faculty, University of Bonab, Bonab, Iran. M. Zarrebini is with the Department of Textile Engineering, Isfahan University of Technology, Isfahan, Iran. Correspondence should be addressed to R. Saghafi (e-mail: Saghafi@bonabu.ac.ir).

0, 45 and 90 degrees.

Radon transform function was applied to the simulated images. Fig. 2 shows the model image at an angle of 45° and its relevant Radon transform.

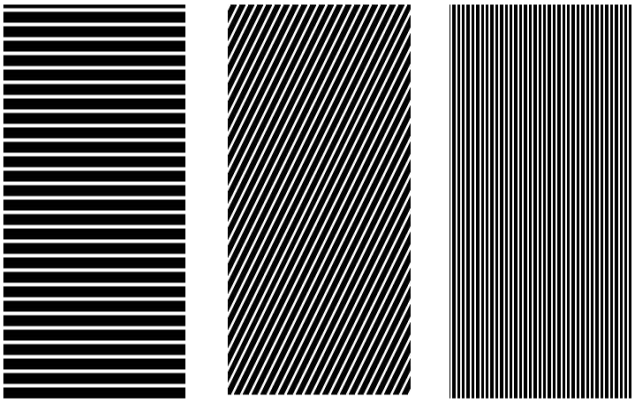

Fig. 1. Three simulated images at different angles.

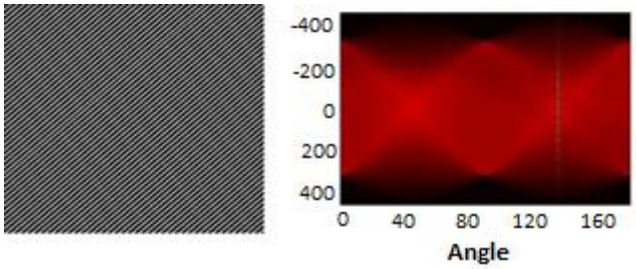

Fig. 2. Simulated image with lines at 45° and its color Radon transformation histogram.

Bright points along the vertical Radon transform image must be considered to be at 135° direction. The chart with a peak at 135°, shown in Fig. 3 was constructed by selecting the rows of Radon transform matrix with the largest numbers and arranging them in a 1° increment from 1° to 180°. Since there is a phase lead of 90° between the Radon orientation angle and the true orientation, the following equation can be deduced:

True orientation angle = (1)

Random orientation angle -90

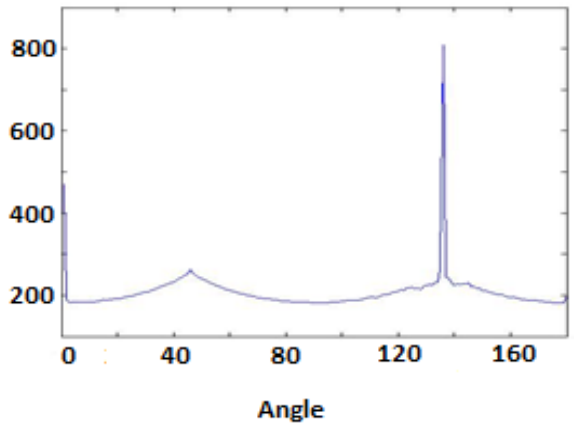

Fig. 3. Chart of larger numbers in the transform matrix in the range of 1° to 180°.

Therefore, orientation function $f(\alpha)$ which shows the difference in orientation between α_1 and α_2 angles can be deduced. Properties of the orientation function are represented by the following equation:

$$f(a+\pi) = f(a+) \quad and \quad \int_0^{\pi} f(a)da = 1 \tag{2}$$

C. Fiber Orientation Measurement Using Radon Transform Method

Radon transform method was used to evaluate the fiber orientation of the needle punched samples. The face side lighting technique was chosen for imaging. Two LED light sources were positioned at a 45° angle in relation to the face side of the fixed samples. A microphotograph of the needle punched sample was taken at 2x optical zoom using a CCD camera. A series of 600×600 pixels and 72 dpi images were prepared. Images were composed of 256 grey levels. Binary transformation of images was delicately carried out using binary format equation:

$$B_i = mean - \frac{SD}{2} \tag{3}$$

where "*Bi*" and "*mean*" define the binary threshold and the average numerical value of microphotograph, respectively. *SD* is the standard deviation of the microphotograph pixels value.

Fiber orientation chart of the samples was constructed using the algorithm shown in Fig. 4. The binary image of a sample and its fiber orientation chart were obtained using Radon transformation as illustrated in the Fig. 5. The mean fiber orientation angle can be calculated from the orientation chart using flowing equation:

$$M(a) = \left(\frac{\sum_{a=0}^{a=90} f(a)\times a}{\sum_{a=0}^{a=90} f(a)} + \frac{\sum_{a=0}^{a=180} f(a)\times(180-a)}{\sum_{a=0}^{a=90} f(180-a)}\right)/2 \tag{4}$$

where *M(α)* is the mean fiber orientation angle and *f(α)* is the difference in orientation between two angles α_n and α_{n+10}.

D. Bending Properties Determination Using Two Simply Supported Beam System Method

The bending modulus of samples was determined using two simply supported beam system as shown in Fig. 6 [10]. In the case of a beam deformed under an applied load, the bending moment varies along the length of the beam. Thus, the curvature along the beam changes with variations in the bending moment. In beams with rectangular cross-section, by assuming that there is no change in the cross-section during the application of the load, the bending modulus can be calculated using Eq. (5).

$$E = \frac{wl^3}{4Ybh^3} \tag{5}$$

where, *E is* the bending modulus, *Y* denotes the beam deformation, and *L*, *w*, *b*, and *h* represent the length of the

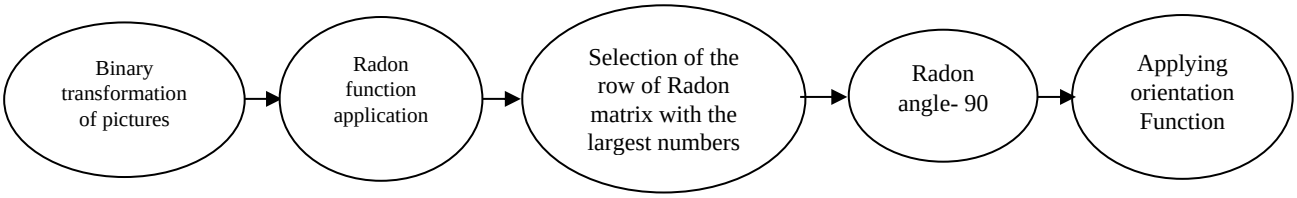

Fig. 4. Schematic representation of fiber orientation determination using Radon transform algorithm.

beam, the applied load, the width and the thickness of the rectangular sample, respectively. In this work a Zwick 1446-60 tensile tester machine was used to evaluate the bending stiffness of the needled samples. In order to test the sample a U-shaped metallic piece was made. The distance between the two tines of the U-shaped piece was set at 5 cm. The U-shaped piece was fixed to the lower jaw. A sharp edge metallic plate, as shown in Fig. 6, was fixed to the upper jaw. Samples of 6 × 2.5 cm from needle-punched fabrics were prepared. The test sample was placed on the tines of the U-shape piece. The tensile tester was set to operate in the compressive mode. As the lower jaw moved upwards, the sharp edge of the metallic plate pressed downwards on the middle of the sample. The deflecting force was both sensed and measured by the tensile tester. The amount of the upward movement of the lower jaw, labeled as crush in the diagrams of the Zwick tester, was a measure of the deflection in the middle of the bent test samples.

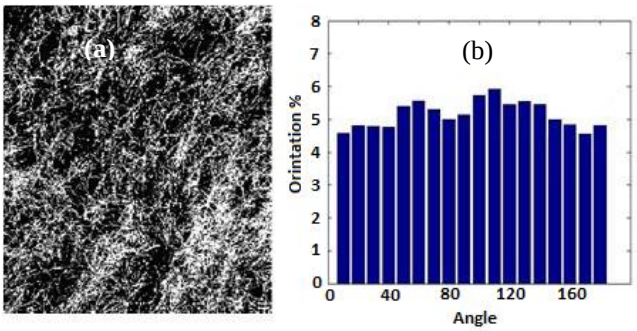

Fig. 5. (a) Binary image of a needle punched sample, (b) Orientation chart based on Radon method.

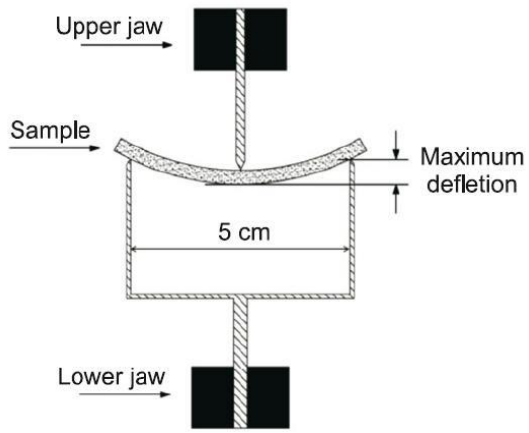

Fig. 6. A schematic diagram of a tensile tester adopted for bending tests [10].

E. Strength Breaking Measurement Using Strip Method

The breaking strength of the samples was determined using strip method [9]. Ten 20.5×220 mm samples were cut. The Zwick 1446-60 tensile tester machine was used to evaluate the breaking strength of the needle-punched samples. For all the tensile experiments, the crosshead speed and the jaws gap were 10 mm min^{-1} and 150 mm, respectively.

TABLE I
CALCULATED BENDING MODULUS (**BM**) OF THE SAMPLES IN TERMS OF PUNCH DENSITY **(PD)** AND NEEDLE PENETRATION DEPTH (**NP**)

fabric weight ($g\ m^{-2}$)	direction[a]	NP (mm)	BM ($kg\ cm^{-2}$)				
			PD=31[b]	PD =42[b]	PD =51[b]	PD =60[b]	PD=66[b]
200	A	0	0.114	0.114	0.114	0.114	0.114
		7	0.128	0.151	0.167	0.182	0.219
		13	0.189	0.224	0.247	0.269	0.324
		20	0.324	0.385	0.424	0.462	0.556
300	A	0	0.113	0.113	0.113	0.113	0.113
		7	0.154	0.167	0.172	0.188	0.225
		13	0.227	0.246	0.254	0.277	0.332
		20	0.537	0.582	0.601	0.655	0.786
400	A	0	0.121	0.121	0.121	0.121	0.121
		7	0.158	0.174	0.179	0.185	0.202
		13	0.395	0.479	0.493	0.509	0.555
		20	0.567	0.688	0.708	0.731	0.797
500	A	0	0.088	0.088	0.088	0.088	0.088
		7	0.112	0.126	0.142	0.157	0.161
		13	0.397	0.515	0.580	0.640	0.657
		20	0.525	0.681	0.767	0.846	0.869
200	T	0	0.106	0.106	0.106	0.106	0.106
		7	0.134	0.166	0.184	0.197	0.236
		13	0.188	0.233	0.258	0.277	0.331
		20	0.241	0.299	0.331	0.355	0.425
300	T	0	0.088	0.088	0.088	0.088	0.088
		7	0.132	0.150	0.155	0.223	0.237
		13	0.225	0.256	0.265	0.381	0.405
		20	0.538	0.612	0.634	0.912	0.969
400	T	0	0.104	0.104	0.104	0.104	0.104
		7	0.132	0.155	0.171	0.193	0.203
		13	0.346	0.472	0.521	0.588	0.618
		20	0.543	0.740	0.817	0.922	0.969
500	T	0	0.058	0.058	0.058	0.058	0.058
		7	0.078	0.102	0.115	0.130	0.133
		13	0.385	0.502	0.568	0.641	0.659
		20	0.569	0.742	0.839	0.947	0.973

[a] The letter codes "A" and "T" denote the machine and cross-machine direction, respectively.
[b] per cm^2

III. Results and Discussion

A. Mechanical Properties of the Fabrics

The bending modulus of the samples in terms of punch density and needle penetration depth for each weight group are shown in Table I.

TABLE II
CALCULATED BREAKING STRENGTH (**BS**) OF THE SAMPLES IN TERMS OF PUNCH DENSITY (**PD**) AND NEEDLE PENETRATION DEPTH (**NP**)

fabric weight ($g\ m^{-2}$)	direction[a]	NP (mm)	BS ($kg\ m\ s^{-2}$)				
			PD=31[b]	PD =42[b]	PD =51[b]	PD =60[b]	PD=66[b]
200	A	0	8.82	8.82	8.82	8.82	8.82
		7	22.35	25.26	27.53	27.90	28.35
		13	48.93	55.30	60.27	61.08	62.07
		20	79.84	90.23	98.35	99.66	101.28
300	A	0	19.27	19.27	19.27	19.27	19.27
		7	15.64	17.68	47.60	48.23	49.02
		13	102.55	115.89	126.33	128.01	130.09
		20	193.74	218.94	238.65	241.83	245.76
400	A	0	32.36	32.36	32.36	32.36	32.36
		7	77.32	79.16	86.82	86.53	84.62
		13	293.59	300.54	329.64	330.75	338.20
		20	377.64	386.59	424.02	425.45	435.04
500	A	0	43.55	43.55	43.55	43.55	43.55
		7	112.56	133.48	135.07	145.72	159.88
		13	364.65	432.40	437.56	472.05	517.93
		20	494.13	585.93	592.92	639.66	701.83
200	T	0	5.49	5.49	5.49	5.49	5.49
		7	10.61	12.92	13.71	18.11	21.36
		13	26.42	32.17	34.15	45.10	53.20
		20	60.58	73.77	78.30	103.42	121.99
300	T	0	6.52	6.52	6.52	6.52	6.52
		7	18.06	21.83	23.17	30.60	36.10
		13	56.10	67.79	71.96	95.04	112.11
		20	155.45	187.83	199.38	263.33	310.62
400	T	0	8.02	8.02	8.02	8.02	8.02
		7	21.62	29.65	32.14	35.41	38.42
		13	149.49	205.02	222.21	244.80	265.61
		20	219.03	300.40	325.59	358.68	389.18
500	T	0	11.15	11.15	11.15	11.15	11.15
		7	40.64	44.03	51.35	58.17	70.06
		13	207.98	225.33	262.79	297.72	358.55
		20	313.71	339.88	396.38	449.06	540.82

[a] The letter codes "A" and "T" denote the machine and cross-machine directions, respectively.
[b] per cm^2

In order to determine the effect of punch-density and needle penetration on the mechanical properties of needled samples in both principle directions, statistical analyses of the data both dependently and independently were carried out and their significance at 95% confidence limit was confirmed. The results showed that, in general, an increase in the amount of punch-density and needle penetration depth during the needling operation led to higher bending modulus in both principle directions. However, the rate of the increase in bending modulus of the sample in the machine-direction was higher than that of the cross machine-direction.

The calculated values of breaking strength of the samples in terms of punch density and needle penetration depth for each weight groups is shown in Table II.

Results point to existence of the similar effect on breaking strength of the samples by amount of punch-density and needle penetration depth as with the bending modulus. It is found that the fabrics with higher weights exhibit higher tensile strength. This is due to the presence of more fibers in the in the cross-section of the fabrics. Results also pointed to the fact that breaking strength of the samples in the machine-direction is higher than that in the cross-machine direction. As is explained in section *C*, the majority of the fibers are oriented approximately along the machine-direction. Hence during tensile test in the machine-direction, these fibers can readily re-orient and lie in the direction of the applied force. The results also show that, an increase in the amount of punch density and needle penetration depth in general improves the breaking strength of the samples in both principle directions. However, samples experience a higher rate of increase in breaking strength in the machine-direction than in the cross-machine direction.

TABLE III
MEAN FIBER ORIENTATION ANGLE (**MFO**) OF THE SAMPLES IN TERMS OF PUNCH DENSITY (**PD**) AND NEEDLE PENETRATION DEPTH (**NP**)

fabric weight ($g\ m^{-2}$)	NP (mm)	MFO (°)				
		PD=31[a]	PD =42[a]	PD =51[a]	PD =60[a]	PD=66[a]
200	0	50.82	50.82	50.82	50.82	50.82
	7	51.07	51.99	52.83	53.82	54.59
	13	51.47	52.34	53.21	54.07	54.94
	20	50.82	50.82	50.82	50.82	50.82
300	0	51.14	51.14	51.14	51.14	51.14
	7	51.43	52.03	52.61	53.214	53.79
	13	51.65	52.15	52.65	53.36	53.85
	20	51.07	51.77	52.42	53.09	53.30
400	0	51.47	52.34	53.21	54.07	54.94
	7	51.47	51.47	51.47	51.47	51.47
	13	52.17	52.78	53.37	53.98	54.57
	20	52.20	52.89	53.52	54.13	54.73
500	0	51.58	51.58	51.58	51.58	51.58
	7	52.24	52.75	53.44	54.45	54.64
	13	52.37	52.88	53.59	54.70	54.90
	20	51.89	52.30	53.26	54.20	54.63

[a] per cm^2

B. Fiber Orientation as Determined by Radon Transforms Method

The results of the mean fiber orientation angle of the samples according to changing the punch-density and needle penetration depth for different weights are shown in Table III.

Multiple regressions were used to investigate the effect of the sample weight, penetration depth and punch density on mean fiber orientation angle of the samples. Needle

penetration depth (X_{dp}), punch density (X_{npd}) and weight (X_{fw}) are the independent variables and mean fiber orientation angle (Y_{foa}) is the dependent variable. Fitting of a Quadratic regression model to these data yielded Eqs. (6) and (7).

$$Y_{foa} = 48.1391 + 0.0165 \times X_{fw} + 0.1088 \times X_{dp} - 0.00002 \times X^2_{fw} - 0.0022 \times X^2_{dp} \quad (6)$$

$$Y_{foa} = 49.4479 + 0.0060 \times X_{fw} + 0.0359 \times X_{npd} - 0.00009 \times X^2_{fw} + 0.0004 \times X^2_{npd} \quad (7)$$

Fig. 7 shows the multiple regression pictorial representation of mean fiber orientation angle against fabric weight, depth of penetration and punch density.

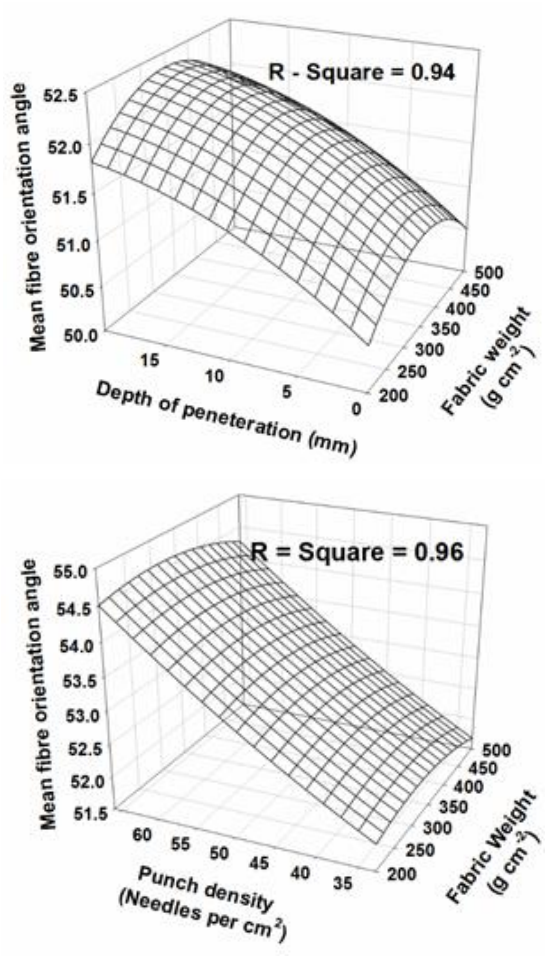

Fig. 7. The effect of punch-density, needle penetration depth and sample weight on mean fiber orientation angle of the samples.

Multiple regressions were also used to investigate the correlation between needle penetration depth (X_{dp}) and punch density (X_{npd}) as independent variables and mean fiber orientation angle (Y_{foa}) as dependent variable at various fabric weights. Fitting of a quadratic regression model to these data yielded Eqs. (8) to (11).

Fig. 8 shows the multiple regression pictorial representation of mean fiber orientation angle against punch density and depth of penetration in various fabric weights**.**

$$Y_{foa} = 47.20 + 0.1 \times X_{npd} + 0.12 \times X_{dp} + 0.00003 \times X^2_{npd} - 0.006 \times X^2_{dp} \quad (8)$$

$$Y_{foa} = 48.87 + 0.07 \times X_{npd} + 0.09 \times X_{dp} + 0.000007 \times X^2_{npd} - 0.004 \times X^2_{dp} \quad (9)$$

$$Y_{foa} = 49.58 + 0.05 \times X_{npd} + 0.13 \times X_{dp} + 0.0002 \times X^2_{npd} - 0.006 \times X^2_{dp} \quad (10)$$

$$Y_{foa} = 50.08 + 0.02 \times X_{npd} + 0.12 \times X_{dp} + 0.0006 \times X^2_{npd} - 0.006 \times X^2_{dp} \quad (11)$$

As can be seen an increase in the amount of punch-density leads to an increase in mean fiber orientation angle in all samples along the machine-direction. This is due to the displacement of the fibers by the needling process. Additionally, fiber orientation pattern of the samples enormously changes due to changes in needle penetration depth. An increase in the needle penetration leads to an increase in mean fiber orientation angle of the samples up to a maximum value beyond which the mean fiber orientation angle decreases. These results reveal that in high penetration depths, displacement of the fibers by the needling process will be reduced. This is maybe due to the enhancement of entanglement in fibrous webs. Multiple regression analysis also points to effective influence of punch density and needle penetration depth on mean fiber orientation angle of the samples. High value of R^2 shows the importance of the effect of needling parameters on fiber orientation pattern of the samples.

C. Effect of Mean Fiber Orientation and Fabric Weight on Mechanical Properties of the Fabrics

Plane regression model method was used to investigate the effect of mean fiber orientation and fabric weight on the mechanical properties of the samples. This was achieved by considering the mean fiber orientation angle (X_{foa}) and the fabric weight (X_{fw}) of the samples as independent parameters that affect bending modulus ($Y_{bm(md)}$) and ($Y_{bm(cmd)}$) in the machine and the cross-machine directions, respectively. Fig. 9 shows the multiple regression pictorial representation of bending modulus in principle directions against fabric weight and mean fiber orientation angle. The fitting of plane regression models to these data yielded Eqs. (12) and (13).

$$Y_{bm(md)} = -3.568 + 0.001 \times X_{fw} + 0.067 \times X_{foa} \quad (12)$$

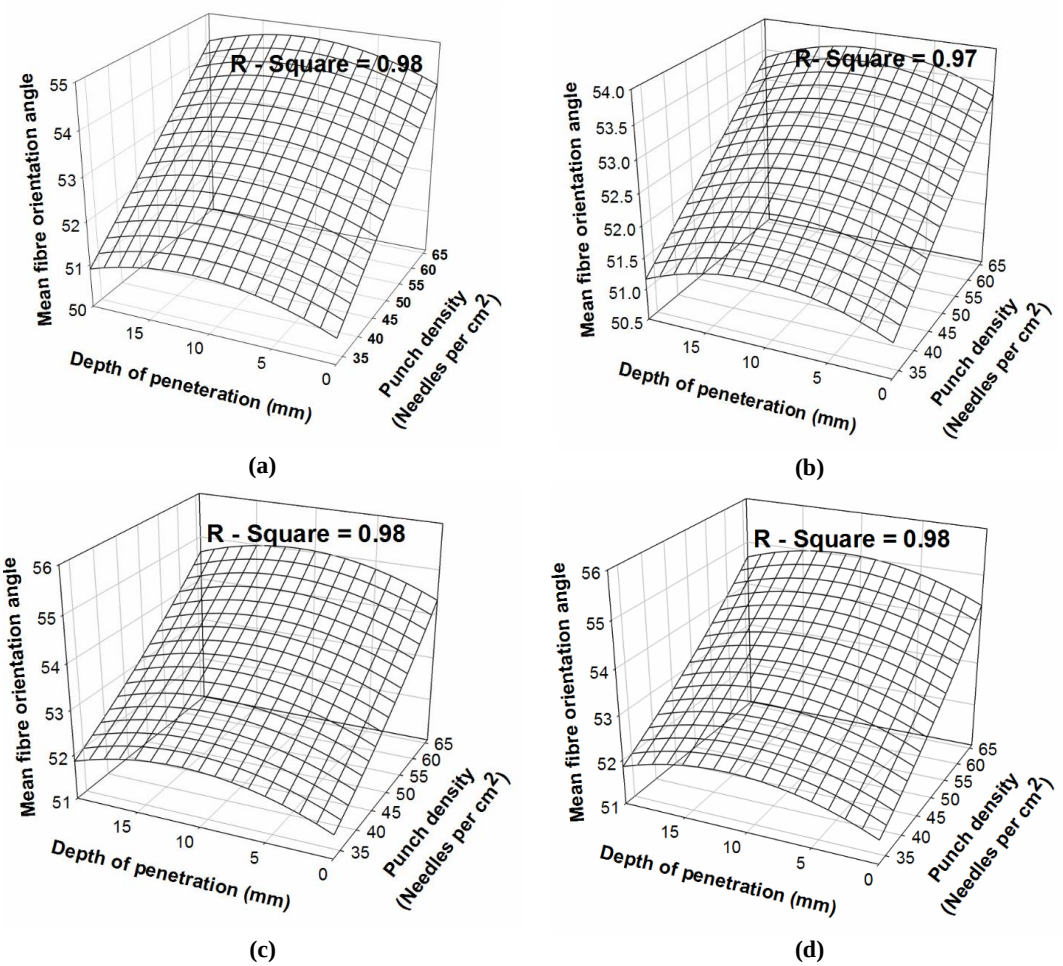

Fig. 8. The effect of punch-density and needle penetration depth on mean fiber orientation angle of the samples (a) 200 g, (b) 300 g , (c) 400 g and (d) 500 g.

$$Y_{bm(cmd)} = -4.05 + 0.001 \times X_{fw} + 0.076 \times X_{foa} \quad (13)$$

The results show that, an increase in the weight and mean fiber orientation angle of the samples causes the bending modulus in both principle directions to increase. However, the amount of increase in bending modulus in the machine-direction is higher than that in the cross-machine direction. This is due to displacement of fibers by needling process. The coefficient of determination (R^2) of the above equations is 0.9 and 0.89, respectively. This emphasizes the importance of the effect of mean orientation angle and fabric weight on the bending modulus of the samples.

Fig. 10 shows the multiple regression pictorial representation of breaking strength in the machine direction ($Y_{bs(md)}$), and the cross-machine direction

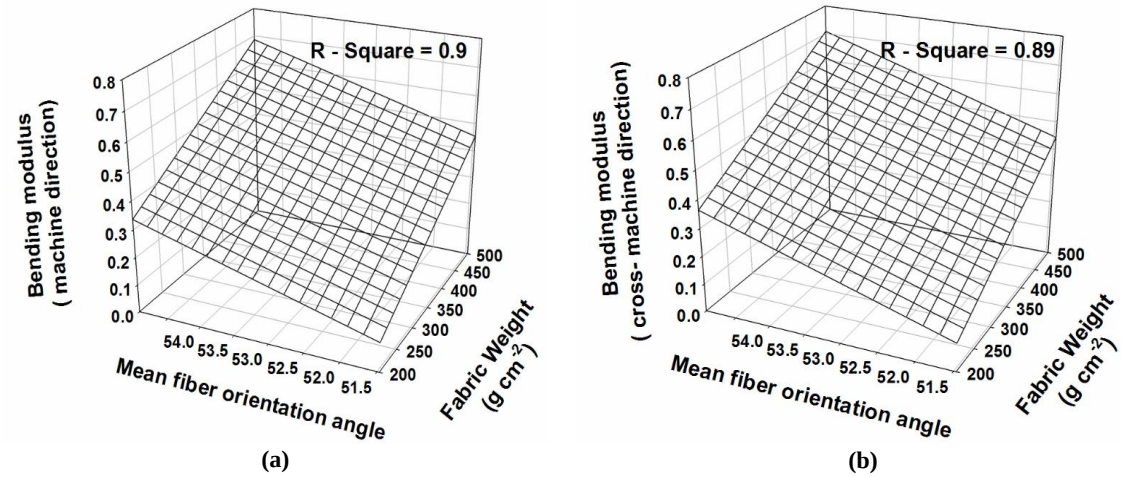

Fig. 9. Effect of fabric weight and mean fiber orientation angle of the samples on bending modulus in the principle directions.

($Y_{bs(cmd)}$), when the mean fiber orientation angle (X_{foa}) and the fabric weight (X_{fw}) are considered to be the independent variables affecting the breaking strength of the samples. Fitting of plane regression models to these data yielded Eqs. (14) and (15).

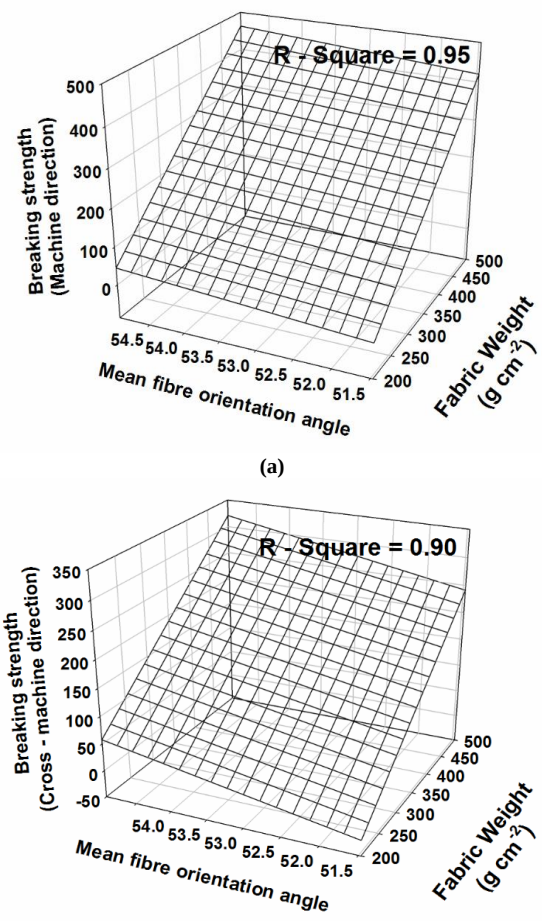

Fig. 10. Effect of fabric weight and mean fiber orientation angle of the samples on breaking strength in principle directions.

$$Y_{bs(md)} = -914.192 + 1.393 \times X_{fw} + 12.395 \times X_{foa} \quad (14)$$

$$Y_{bs(cmd)} = -1376.356 + 0.878 \times X_{fw} + 22.906 \times X_{foa} \quad (15)$$

The results show that, breaking strength in both principle directions occurs due to an increase in weight and mean fiber orientation angle of the samples. However, in comparison to cross-machine direction, increase in breaking strength in the machine-direction is not only more but is also faster. Majority of the fibers are oriented at angles approximately along the machine-direction. Hence during the tensile test in the machine-direction, these fibers can readily re-orient and lie in the direction of the applied force. High value of R^2 shows the importance of the effect of fiber orientation and fabric weight on breaking strength of the samples. The results point to the paramount importance of the degree of fiber orientation and fabric weight as two influential factors controlling the mechanical properties of the needle punched fabrics.

IV. Conclusion

This research revealed that fiber orientation in webs is an important factor that affects the fabric tensile properties. The results showed that an increase in the amount of punch density led to re-orientation of more fibers in the machine-direction. This was attributed to the displacement of fibers by the needling process. Additionally, fiber orientation pattern of the samples was enormously affected by the variations in the needle penetration depth. It was observed that an increase in the needle penetration depth caused the mean fiber orientation to increase to a maximum beyond which further increase in the needle penetration caused the mean fiber orientation to decrease. These results revealed that in high penetration depths, displacement of the fibers by the needling process would be reduced. This was maybe due to the enhancement of entanglement in fibrous webs.

Multiple regression analysis pointed to the significant effect of punch density and needle penetration depth on mean fiber orientation angle of the samples. Results also showed bending modulus of the samples in the both machine and cross-machine directions could be increased by an increase in punch density and needle penetration depth. However, bending modulus in the machine-direction increases at a higher rate in comparison to that in the cross-machine direction. It was concluded that the properties of needled fabrics are greatly influenced by needling parameters and fiber distribution. High values of (R^2) showed the importance of the effect of fiber orientation and fabric weight on breaking strength and bending modulus of the samples. Fiber distribution and fabric weight in needled fabrics were found to be the influential factors controlling the fabric mechanical properties. It is concluded that the requirements of needle-punched fabric end uses can be met using the results of this research.

Acknowledgment

The authors would like to express their sincere thanks to the deputy of research of University of Bonab for the financial and technical support.

References

[1] B. Goswami, T. Beak, and F. L. Scardino, "Influence of Geometry on the Punching-Force Characteristics of During Needle Felting", *Text. Res. J.*, vol. 42, no. 10, pp. 605-612, 1972.

[2] B. Pourdeyhimi, R. Ramanathan, and R. Dent, "Measurement of Fiber Orientation in Nonwovens, Part 1: Simulation", *Text. Res. J.*, vol. 66, no. 11, pp. 713-722. 1996.

[3] B. Pourdeyhimi, R. Ramanathan, and R. Dent, "Measurement of Fiber Orientation in Nonwovens, Part 2: Direct Tracking", *Text. Res. J.*, vol. 66, no. 12, pp. 747-753, 1996.

[4] B. Pourdeyhimi, R. Ramanathan, and R. Dent, R. Measurement of Fiber Orientation in Nonwovens, Part 3: Fourier Transform", *Text. Res. J.*, vol. 67, no. 2, pp. 143-151, 1997.

[5] B. Pourdeyhimi, R. Ramanathan, and R. Dent, "Measurement of Fiber Orientation in Nonwovens, Part 4: Flow Filed Analysis", *Text. Res. J.*, vol. 67, no. 3, pp. 181-187, 1997.

[6] B. Pourdeyhimi , R. Ramanathan, and R. Dent, "Measurement of Fiber Orientation in Nonwovens, Part 5: Real webs". *Text. Res. J.*, vol. 69, no. 3, pp. 185-192, 1999.

[7] X. Bugao and Y. Ling, "Determining Fiber Orientation Distribution

in Nonwovens with Hough Transform Technique", *Text. Res. J.*, vol 67, no. 8, pp. 563-571, 1999**.**

[8] ASTM D5035-95 Standard Test Method for Breaking Force and Elongation of Textile Fabrics (Strip Method).

[9] Data of matlab toolbox. available : http://matlab.izmiran.ru/help/toolbox/images/transfo8.html

[10] M. Ghane, R. Saghafi, M, Zarrebini, and D. Semnani, "Evaluation of Bending Modulus of Needle-Punched Fabrics Using Two Simply Supported Beam Method", *Fibres Text. East. Eur.*, vol. 19, no. 1, pp. 89-93, 2011.